

Electrical and magnetic properties of conductive Cu-based coated conductors

T. Aytug,^{a),b)} M. Paranthaman, J. R. Thompson,^{a)} A. Goyal, N. Rutter, H. Y. Zhai, A. A. Gapud, A. O. Ijaduola,^{a)} and D. K. Christen
Oak Ridge National Laboratory, Oak Ridge, Tennessee 37831

(Received 11 June 2003; accepted 17 September 2003)

The development of $\text{YBa}_2\text{Cu}_3\text{O}_{7-\delta}$ (YBCO)-based coated conductors for electric power applications will require electrical and thermal stabilization of the high-temperature superconducting (HTS) coating. In addition, nonmagnetic tape substrates are an important factor in order to reduce the ferromagnetic hysteresis energy loss in ac applications. We report progress toward a conductive buffer layer architecture on biaxially textured nonmagnetic Cu tapes to electrically couple the HTS layer to the underlying metal substrate. A protective Ni overlayer, followed by a single buffer layer of $\text{La}_{0.7}\text{Sr}_{0.3}\text{MnO}_3$, was employed to avoid Cu diffusion and to improve oxidation resistance of the substrate. Property characterizations of YBCO films on short prototype samples revealed self-field critical current density (J_c) values exceeding 2×10^6 A/cm² at 77 K and good electrical connectivity. Magnetic hysteretic loss due to Ni overlayer was also investigated. © 2003 American Institute of Physics. [DOI: 10.1063/1.1626263]

Potential applications of high-temperature superconducting (HTS) coated conductors involve the electric utility and power industries.^{1,2} For effective implementation at cryogenic temperatures (~ 30 –77 K), stabilization against thermal runaway will be required in the event of an overcurrent situation (exceeding critical current I_c of the HTS coating). In general, a coated conductor architecture involves epitaxial fabrication of a thin layer (1–2 μm) of HTS film [usually $\text{YBa}_2\text{Cu}_3\text{O}_{7-\delta}$ (YBCO)] on biaxially textured buffer layers deposited on a thick (50 μm) flexible metal substrate (Ni or dilute Ni alloys). Thus, additional stabilization by electrical connection to a good conductor is required for insulating buffer layers and resistive Ni alloy substrates ($> 10 \mu\Omega$ cm at 77 K).^{3–5} A solution is to electrically shunt the HTS layer either by an intermediate conductive buffer layer to a low-resistive metal substrate (i.e., Ni or Cu)^{3,4} or by depositing a stabilizing metallic cap layer (i.e., Cu or Ag) onto the HTS coating.⁵ While a conductive buffer provides an effective solution only when the substrate material is highly conductive,^{3–5} it is the most desirable approach from an applications perspective since it would yield the optimum engineering current density J_E (I_c per unit total cross-sectional area).^{5,6} Coupling the HTS layer adequately to a pure Ni or Cu tape through a conductive buffer layer also provides an overall less complicated structure with reduced resistance and an increased thermal conductivity, providing more efficient heat transfer to either a coolant bath or through the thermal diffusivity of the system.^{5,6}

To date, many reports on coated conductor fabrication using the rolling assisted biaxially textured substrates (RABiTS) technique have utilized high-purity Ni (99.99%) and strengthened Ni alloy as the base, textured material. However, the ferromagnetism (FM) of pure Ni and Ni alloy hinders their use in applications requiring time-varying (ac) currents due to hysteretic energy losses. On the other hand,

Cu is a lower cost, lower resistivity, and nonmagnetic alternative for the production of long-length RABiTS-based coated conductor tapes. Recently, we have demonstrated the growth of electrically well-coupled YBCO films on *conductive* $\text{SrRuO}_3/\text{LaNiO}_3$ bilayer and $\text{La}_{0.7}\text{Sr}_{0.3}\text{MnO}_3$ (LSMO) single-layer buffer structures deposited on biaxially textured Ni tapes.^{3,5} Although there has been recent progress in the development of nonconductive, protective buffer architecture,^{7,8} there have been no reports on the development of *conductive* buffer layers on pure Cu substrates for coated conductor applications. Because of its electrical conductivity, thermal stability, and structural compatibility with YBCO, we have investigated the viability of LSMO as a *conductive* buffer interface on biaxially textured Cu substrates. Here, we demonstrate the fabrication of electrically connected high critical current density J_c ($> 2 \times 10^6$ A/cm² at 77 K) YBCO coatings on Cu tapes. The electrical, superconducting, and magnetic (hysteretic loss) properties of these short prototype conductors are reported.

Cube textured $[\{100\}(100)]$ Cu substrates of 50 μm thickness were obtained from randomly oriented high purity (99.99%) Cu bars by cold-rolling, followed by an anneal in vacuum at 800 °C for 1 h. To minimize Cu diffusion and to reduce the oxidation rate of the substrate,⁹ first a protective Ni overlayer (1.6 μm) was deposited by dc-magnetron sputtering at a temperature of 600 °C in a reducing atmosphere of forming gas (96% Ar+4% H₂). Subsequent growth of the LSMO buffer was conducted by rf-magnetron sputtering in a mixture of forming gas and 2×10^{-5} Torr of H₂O, with the substrate temperature at 550–625 °C. These conditions have solved the slight Sr contamination that we have observed in earlier work of LSMO on Ni.⁴ The YBCO films were grown at 780 °C in 120 mTorr of O₂ by pulsed-laser deposition using a KrF excimer laser system operated at an energy density of ≈ 2 J/cm². For these research samples, typical thicknesses of the LSMO and the YBCO films were 300 and 200 nm, respectively. The crystallographic orientation and texture of the films were characterized by x-ray diffraction (XRD). A

^{a)}Department of Physics, University of Tennessee, Knoxville, TN 37996.

^{b)}Electronic mail: aytugt@ornl.gov

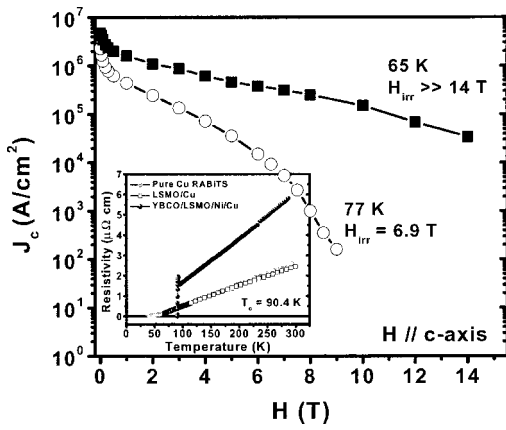


FIG. 1. Magnetic field dependence of J_c curves measured at 65 and 77 K, for a YBCO film on the conducting buffer structure of LSMO/Ni/Cu. The inset shows the temperature-dependent net resistivity of the same YBCO sample, as well as the data for LSMO/Cu and for a pure biaxially textured Cu substrate.

standard four-probe technique was used to evaluate the electrical properties, including the temperature-dependent resistivity of the conductive buffer layers, superconducting transition temperature (T_c), J_c , and $I-V$ characteristics of the composite structure. Values of J_c were assigned at a $1 \mu\text{V}/\text{cm}$ criterion. The magnetic properties of the samples were measured in a superconducting-quantum-interference-device-based magnetometer at a temperature of 95 K, in fields H , up to 800 Oe applied parallel to the tape plane.

Figure 1 shows the J_c performance of a YBCO film deposited on LSMO/Ni/Cu substrate as a function of magnetic field measured at the boiling and near-triple-point temperatures of liquid nitrogen, with the field applied parallel to the c axis. The sample has a $T_c > 90$ K, indicating cation-contamination-free YBCO. At 77 K, the zero-field transport J_c is 2.3×10^6 A/cm² and the irreversibility field (H_{irr}) is high, near 7 T. At 65 K, J_c is 4.8×10^6 A/cm² and remains around 1×10^6 A/cm² at 3 T, which is highly desirable for applications such as motors, generators and energy storage requiring field strengths of several tesla. Note that these high J_c values could be obtained primarily due to the excellent texture, with low-angle grain-to-grain correlations dominating the entire sample and an overall high degree of in-plane ($\Delta\phi$) and out-of-plane ($\Delta\omega$) alignment. In fact, the measured XRD full width at half-maximum (FWHM) widths $\Delta\phi$ and $\Delta\omega$ of the average total ensemble of grains are sharp; 7° and 6.5° for YBCO, and 6° and 5° for underlying Cu substrate, respectively. It is clear from the inset of Fig. 1, showing the temperature-dependent four-point resistivity measurements, that there is excellent electrical coupling between the Cu substrate and the LSMO layer, as evidenced by the similar $\rho_{net}-T$ behaviors. However, after the YBCO deposition, $\rho_{net}-T$ characteristics of the sample deviates from the ideal behavior, indicating somewhat degraded metallic connectivity, most likely resulting from the presence of discontinuous NiO regions (detected from the XRD analysis) at the LSMO-Ni interface. In fact, our model calculations showed that the observed increase in ρ_{net} at the superconducting transition can be associated with a significant interfacial contact resistance between the YBCO film and the Cu substrate. On the other hand, complete isolation of YBCO from the substrate would yield a ρ_{net} (calculated for the entire structure)

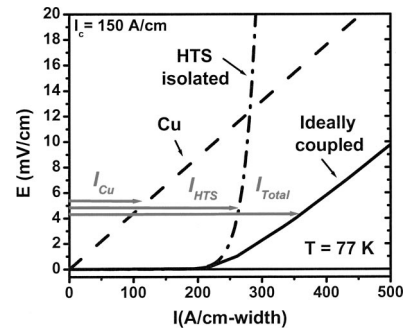


FIG. 2. Ideal current versus electric field characteristics for a model conductor architecture. Data for Cu, electrically isolated HTS, and for the same HTS layer electrically connected to the underlying Cu substrate are compared. Arrows indicate the current sharing among layers for a specific electric field criterion.

that is 2×10^4 times higher than the present value of ρ ($2 \mu\Omega \text{ cm}$) at the transition regime. The observed value is low enough to provide significant stabilization for the current levels of the present structure.

Next, we compare in Fig. 2 the $I-V$ characteristics at 77 K of a model, ideally coupled conductor architecture (HTS+conductive buffer+substrate) with experimental results from the actual sample in Fig. 3. Figure 2 (model) plots I versus electric field ($\text{V}/\text{distance}$ between voltage taps) curves for the Cu tape only, for the isolated HTS coating with an I_c of 150 A/cm width (practical level of operating current), and for the combined ideal case in which the HTS layer and Cu are electrically connected through an intermediate conductive buffer layer. The interfacial contact resistance is assumed to be negligible (i.e., $< 10^{-8} \Omega \text{ cm}^2$). Notice the typical nonlinear $I-E$ behavior for the isolated HTS layer having power law relation $E \propto (I/I_c)^n$. For $I > I_c$, the ideal case exhibits a near-linear differential ohmic behavior, with slope determined by the metal tape resistivity. Then, for an envisioned transient with $I > I_c$, the total current through the conductor partitions between the HTS layer and the metal tape, greatly reducing the power excursion in the entire structure. The $I-V$ curves obtained from our actual sample are displayed in Fig. 3. While the scales are quantitatively different, qualitatively, we observe similar $I-V$ characteristic compared to the model conductor, although the interfacial resistivity is non-negligible, as noted earlier. In order to check the stabilization provided by the metal tape and to push the current to levels greater than I_c , we recorded the data at 1 T and compared that with the data compiled from

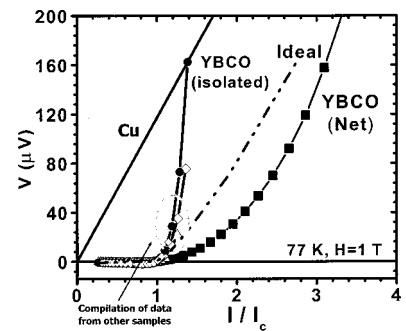


FIG. 3. The $I-V$ curves obtained from the actual sample in a field of 1 T. Figure includes curves for Cu, isolated YBCO films, and data from the YBCO/LSMO/Ni/Cu sample. The dashed line displays the response if there were a complete electrical coupling.

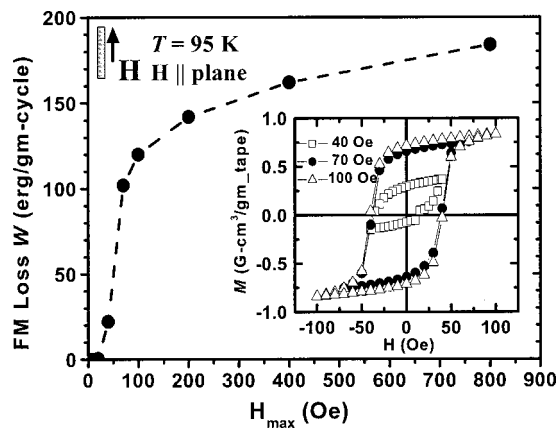


FIG. 4. Ferromagnetic hysteretic loss, W , due to the Ni layer in YBCO/LSMO/Ni/Cu. Note that W first increases rapidly with H_{\max} , then saturates. The inset shows the magnetization loops for the same sample at $T=95$ K, for various H_{\max} excursions, where the field is applied parallel to the plane of the tape.

three other isolated YBCO films having similar power law behaviors. While the results exhibit similar $I-V$ characteristics for bare Cu and isolated HTS film (compared with Fig. 2), data obtained from the actual sample does not agree quantitatively with the ideal behavior (dashed curve). This may be explained by the inhomogeneous electrical coupling and current transfer between the YBCO and the Cu substrate, possibly due to the formation of a discontinuous NiO layer at the interface. Nevertheless, were there a complete isolation, the superconductor would have been destroyed at current levels, $I=3I_c$ (see Fig. 3). Currently, we are trying to improve the electrical coupling and implement a detection mechanism that will monitor voltage across the metal tape.

To determine the potential FM ac loss due to the Ni diffusion barrier, we measured the hysteretic magnetic properties of a fully formed coated conductor at $T=95$ K, just above the superconductive T_c . For these Ni materials, the loss properties change little below 95 K. The quasistatic studies were performed on a sample of mass 9.6 gm, with the dc magnetic field oriented parallel to the plane of the tape. This configuration approximates the self-field on the substrate due to current flow in a tape and it minimizes demagnetization effects. After cooling to 95 K in zero applied field, the hysteretic magnetization loop $M(H)$ was measured by sweeping the field from $+H_{\max}$ to $-H_{\max}$ to $+H_{\max}$ in small steps. A numerical integration of the area inside the loop $M(H)$ provides $W=\oint M(H)d(H)$, the FM energy loss per cycle, with maximum magnetic field H_{\max} . The measurements were repeated as a function of H_{\max} up to 800 Oe, since the FM loss increases with ac field amplitude, which is proportional to the peak ac current. The resulting FM loss W per cycle per gram of tape is shown in Fig. 4 as a function of H_{\max} . The inset of this figure shows the magnetization of the sample for several field excursions. At $H_{\max}=\pm 800$ Oe, the loss has nearly saturated at approximately 180 erg/gm of tape per cycle. The calculated maximum FM hysteretic ac loss at 60 Hz for a 1-m-long and 1-cm-wide tape, of thickness 50 μm would be 5.5 mW, compared with 43 mW for the biaxially textured all "Ni-RABiTS" and 8.4 mW for a magnetically reduced Ni-5 at. % W tape. These FM losses of 5–9 mW correspond to modest additions (10%–20%) to the energy losses expected in HTS coating of achievable YBCO-

based conductors.¹⁰ As an example, for an envisioned coated conductor architecture operating at $I_0=I_c$ of 200 A/cm width, applying the Norris theory,¹¹ which is shown to provide a good estimate of ac loss for YBCO-based conductors,¹² the power loss per meter per cycle is $L_c=(\mu_0/2\pi)I_0^2=480$ mW at 60 Hz. For more realistic operation at $I_0=I_c/2$, in which case the loss is smaller by a factor of 17,⁹ the superconductive hysteretic loss component yields a value of $L_c\sim 28$ mW. Obviously, further reducing the total energy loss would be possible either by reducing the thickness of Ni or completely replacing the Ni film by a functional nonmagnetic metal layer. Similarly, the hysteretic loss in HTS can also be decreased by producing conductors with higher I_c that can operate at smaller I_0/I_c , or possibly by geometrical optimization such as subdividing the tape into noninteracting conductors.

This work shows the development of a coated conductor architecture on biaxially textured Cu tapes having a conductive layer sequence of YBCO/LSMO/Ni/Cu. A self-field J_c (77 K) value exceeding 2×10^6 A/cm² was achieved, and electrical characterization suggests good electrical coupling between the YBCO and the Cu substrate. Assessment of the magnetic loss associated with the Ni overlayer shows that it should be small compared with the hysteretic loss in an operational superconductive coating. Although these initial studies were conducted on pure copper, the ultimate implementation will require strengthened tape. In principle, this can be achieved by appropriate alloying and precipitation hardening, which will also retain high electrical conductivity of the tape.

This work was supported by the U.S. Department of Energy, Office of Power Technologies-Superconductivity Program, Office of Energy Efficiency and Renewable Energy. This work was performed at the Oak Ridge National Laboratory, managed by U.T.-Battelle, LLC for the US DOE under Contract No. DE-AC05-00OR22725. Work at UTK was supported in part by OFOSR grant F49620-02-100182.

- ¹D. P. Norton, A. Goyal, J. D. Budai, D. K. Christen, D. M. Kroeger, E. D. Specht, Q. He, B. Saffian, M. Paranthaman, C. E. Klabunde, D. F. Lee, B. C. Sales, and F. A. List, *Science* **274**, 755 (1996).
- ²A. Goyal, D. P. Norton, J. D. Budai, M. Paranthaman, E. D. Specht, D. M. Kroeger, D. K. Christen, Q. He, B. Saffian, F. A. List, D. F. Lee, P. M. Martin, C. E. Klabunde, E. Hatfield, and V. K. Sikka, *Appl. Phys. Lett.* **69**, 1795 (1996).
- ³T. Aytug, B. W. Kang, C. Cantoni, E. D. Specht, M. Paranthaman, A. Goyal, D. T. Verebelyi, D. K. Christen, J. Z. Wu, R. E. Ericson, C. L. Thomas, C.-Y. Yang, and S. E. Babcock, *J. Mater. Res.* **16**, 2661 (2001).
- ⁴T. Aytug, M. Paranthaman, B. W. Kang, S. Sathyamurthy, A. Goyal, and D. K. Christen, *Appl. Phys. Lett.* **79**, 2205 (2001).
- ⁵C. Cantoni, T. Aytug, D. T. Verebelyi, M. Paranthaman, E. D. Specht, D. P. Norton, and D. K. Christen, *IEEE Trans. Appl. Supercond.* **11**, 3309 (2001).
- ⁶Y. Fu, O. Tsukamoto, and M. Furuse, *IEEE Trans. Appl. Supercond.* **13**, 1780 (2003).
- ⁷T. Aytug, A. Goyal, M. Paranthaman, J. R. Thompson, N. Rutter, H. Y. Zhai, and D. K. Christen, *J. Mater. Res.* **18**, 872 (2003).
- ⁸C. Cantoni, D. K. Christen, M. Varela, J. R. Thompson, and S. J. Pennycook (unpublished).
- ⁹U. V. Aniekwe and T. A. Utigard, *Can. Metall. Q.* **38**, 277 (1999).
- ¹⁰J. R. Thompson, A. Goyal, D. K. Christen, and D. M. Kroeger, *Physica C* **370**, 169 (2002).
- ¹¹W. T. Norris, *J. Phys. D* **3**, 489 (1970).
- ¹²H. R. Kerchner, D. P. Norton, A. Goyal, J. D. Budai, D. K. Christen, D. M. Kroeger, E. D. Specht, Q. He, M. Paranthaman, D. F. Lee, B. C. Sales, F. A. List, and R. Feenstra, *Appl. Phys. Lett.* **71**, 2029 (1997).